Journal of the Less-Common Metals, 171 (1991) 321–327

Uniaxial antiferromagnetic ordering in $TbNiSi_2$

P. Schobinger-Papamantellos

Institut für Kristallographie and Petrographie, ETHZ, CH-8092 Zürich (Switzerland)

K. H. J. Buschow

Philips Research Laboratories, 5600 JA Eindhoven (The Netherlands)

(Received February 4, 1991)

Abstract

The magnetic properties of the compound $TbNiSi_2$ were studied by means of magnetic measurements and neutron diffraction. Neutron diffraction experiments made in the paramagnetic regime confirmed the $CeNiSi_2$ structure reported earlier for this compound. Refined atomic position parameters for $TbNiSi_2$ are given. Neutron diffraction measurements performed in the magnetically ordered regime showed that the terbium moments ($8.7\mu_B$ (Tb atom)$^{-1}$) order antiferromagnetically below $T_N = 36.2$ K, with a collinear magnetic structure in the space group *Cm'cm*, the moment direction being along the *c* axis.

1. Introduction

The crystal structure of rare earth compounds of the composition $RNiSi_2$ was determined by Bodak and Gladyshevskii [1] who showed that the $CeNiSi_2$ structure is closely related to the AlB_2 structure and the α-$ThSi_2$ structure. Rare earth silicides and germanides crystallizing in the two latter structure types have been extensively investigated by the present authors in the last few years [2, 3]. It was found that both the silicides and the germanides have a tendency to form off-stoichiometric compounds in which some of the silicon or germanium positions remain unoccupied. Special attention was paid to the vacancy distribution and its effect on the magnetic structure type.

In view of the close structural relationship between the $RNiSi_2$ compounds and the (defect) silicides and germanides of the AlB_2 and α-$ThSi_2$ structure type we have extended our investigation now to the former compounds. Recently it was shown by Francois *et al.* [4] that the $CeNiSi_2$ structure type is adopted by a considerable number of compounds of the general formula RTX_2 where T represents a 3d transition metal and X = Si, Ge or Sn. Also, in this class of compounds there is a tendency to form off-stoichiometric compositions, which has enhanced our interest in these compounds. In the present study we have restricted ourselves to the investigation of the relatively simple case of $TbNiSi_2$ occurring at the stoichiometric composition, leaving the more complicated off-stoichiometric compositions to future investigations.

0022-5088/91/$3.50

2. Experimental procedures and results

The sample $TbNiSi_2$ was prepared by arc melting from starting materials of at least 99.9% purity. After arc melting the sample was vacuum annealed at 800 °C for about 4 weeks. X-ray diffraction showed that after this treatment the sample was single phase. All reflection lines were indexed on the basis of the orthorhombic $CeNiSi_2$ structure type [1]. The lattice constants are $a = 0.382$ nm, $b = 1.603$ nm, $c = 0.395$ nm.

The magnetic properties of the compound $TbNiSi_2$ were studied by means of a superconducting quantum interference device magnetometer in the temperature range 4.2–350 K in a magnetic field strength of up to 20 kOe. Results of these measurements are displayed in Fig. 1. It may be seen from these data that there is a Néel-type transition at $T_N = 35$ K. In the range well above T_N the reciprocal susceptibility χ^{-1} is seen to behave according to the Curie–Weiss law. The effective moment derived from the slope of the $\chi^{-1}(T)$ curve equals $10.1\mu_B$ (Tb atom)$^{-1}$ which is close to the value of $g\{J(J+1)\}^{1/2} = 9.72\mu_B$ expected for Tb^{3+}. The Curie–Weiss intercept θ_p is equal to -5 K.

The neutron diffraction data were obtained from a powdered sample of $TbNiSi_2$ with the double-axis multicounter system at the Saphiz Reactor, Würenlingen. The wavelength used for the data collection equals 0.17059 nm and the step increment of the diffraction angle 2θ was 0.10°. Measurements were made in the paramagnetic range (60 K) as well as in the magnetically ordered range (8 K). All data were corrected for absorption and evaluated by means of the line profile analysis method [5, 6]. The scattering lengths and magnetic form factor used for terbium are from ref. 7 and ref. 8 respectively.

The neutron diffraction diagram taken at 60 K is shown in Fig. 2. The full curves represent the observed neutron intensities. For the refinement procedure these data were corrected for the background contribution. Results of the refinement procedure based on a trial structure corresponding to the $CeNiSi_2$ type [1]

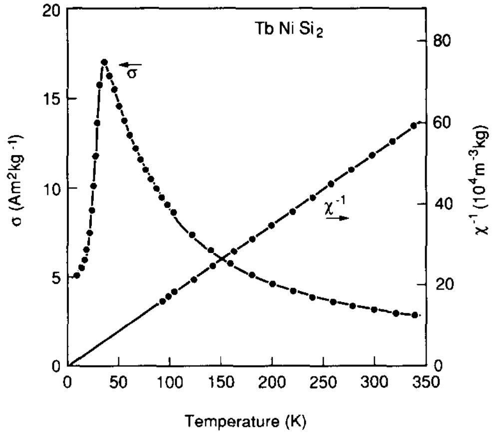

Fig. 1. Temperature dependence of the magnetization σ and temperature dependence of the reciprocal susceptibility χ^{-1} of the compound $TbNiSi_2$.

are represented by the broken lines at the bottom of the figure. The corresponding refined parameters are listed in Table 1.

The neutron pattern obtained at 8 K is shown in Fig. 3. Inspection of the data shows that all magnetic reflections appear at the same reciprocal lattice positions

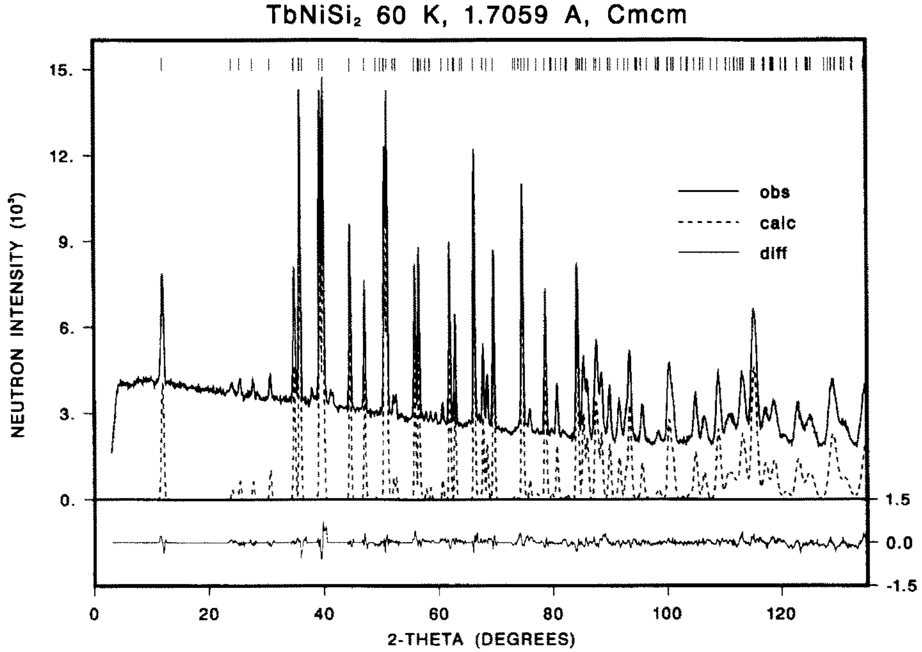

Fig. 2. Neutron diffraction pattern of the compound $TbNiSi_2$ in the paramagnetic range (at 60 K) showing observed intensities (———) and calculated curves (- - -). The differences between observed intensities (corrected for background) and calculated intensities are plotted at the bottom of the figure (——; right-hand scale).

TABLE 1

Refined parameters for the neutron data of $TbNiSi_2$

Temperature (K)	60	8
a (nm)	0.39958(1)	0.39937(1)
b (nm)	1.64041(5)	1.64114(6)
c (nm)	0.39636(1)	0.39606(1)
V (nm^3)	0.25980(2)	0.25959(2)
y_{Tb}	0.1063(1)	0.1063(1)
y_{Ni}	0.3221(1)	0.3219(1)
$y_{Si(1)}$	0.4596(2)	0.4590(3)
$y_{Si(2)}$	0.7495(2)	0.7493(3)
B (nm^2)	0.0022(2)	0.0025(3)
μ/μ_B	—	8.70(4)
R_n, R_m, R_{wp} (%)	4.6, —, 8.5	4.0, 3.1, 7.5
R_{exp} (%), x^2	4.1, 4.2	3.4, 4.9

Space group, *Cmcm*; $Z=4$; all atoms at symmetry site 4c, (0, y, 1/4).

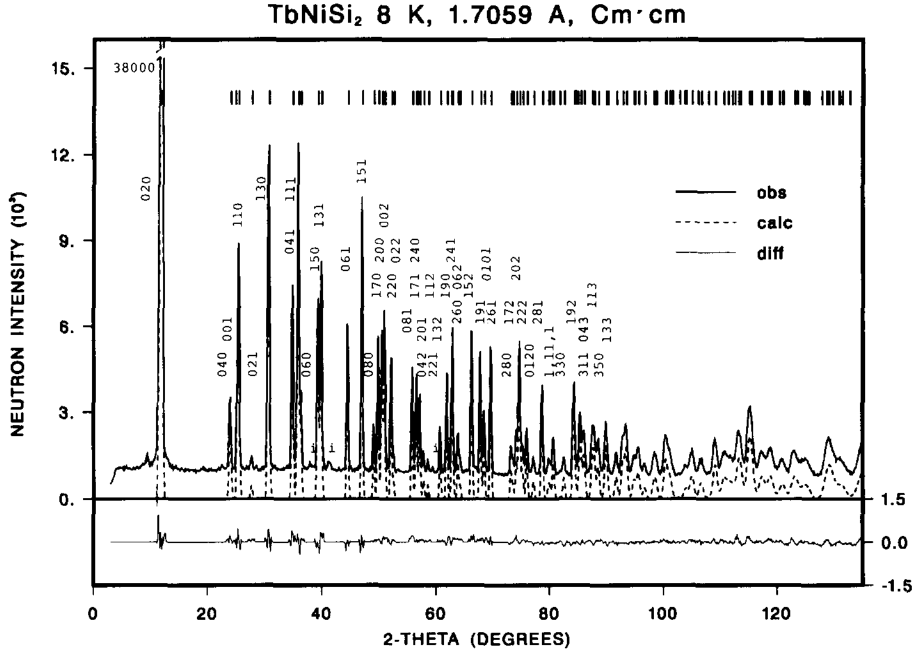

Fig. 3. Neutron diffraction pattern of the compound $TbNiSi_2$ in the antiferromagnetic range (at 8 K) showing observed intensities (———) and calculated curves (- - -). The differences between observed intensities (corrected for background) and calculated intensities are plotted at the bottom of the figure (——; right-hand scale).

as the nuclear reflections, leading to the magnetic wave vector $k = 0$. Owing to the low symmetry of the 4c site (the magnetic atoms being located at the intersection of the mirror planes m_x and m_z and the $2y$ axis) a considerable reduction in the number of free parameters can be achieved by considering the allowed magnetic modes for the eight magnetic space groups [9] associated with $k = 0$ for this site. As may be seen from Table 2, the terbium moments can adopt only a collinear spin arrangement in either the $F(++++)$ or the $G(+-+-)$ mode. Ferromagnetic modes can be ruled out immediately since the magnetic measurements have indicated antiferromagnetic ordering. The easy moment direction of the antiferromagnetic structure has to be along the c axis because of the absence of the allowed magnetic (001) reflection with structure factor $i(1 - 1 + 1 - 1)$. The refinement has confirmed the uniaxial arrangement of the terbium moments according to the magnetic space group $Cm'cm$ (Sh_{63}^{459}). The refined parameters are included in Table 1. The refined moment value of $8.7\mu_B$ indicates that the magnetic moments are slightly below the free ion value $gJ\mu_B = 9\mu_B$ for Tb^{3+}.

The intensity of the magnetic (020) reflection was measured as a function of the temperature. Results are displayed in Fig. 4. The magnetic ordering temperature derived from these data is equal to 36.2 K, which is in good agreement with the Néel temperature obtained from the magnetic measurements.

TABLE 2

Magnetic modes of the 4c symmetry site for the eight possible magnetic space groups of *Cmcm* associated with $k = 0$

Magnetic space group	x	y	z
Cmcm (Sh_{63}^{457})	—	—	—
Cm′cm (Sh_{63}^{459})	—	—	*Gz*
Cmc′m (Sh_{63}^{460})	—	—	—
Cmcm′ (Sh_{63}^{461})	*Gx*	—	—
Cm′c′m (Sh_{63}^{462})	—	—	*Fz*
Cm′cm′ (Sh_{63}^{463})	*Fx*	—	—
Cm′cm′ (Sh_{63}^{464})	—	*Fy*	—
Cm′c′m′ (Sh_{63}^{465})	—	*Gy*	—

$F(++++)$ and $G(+-+-)$ are for the spin signs of terbium atoms (1) $(0, y, 1/4)$, (2) $(0, -y, 3/4)$, (3) $(1/2, 1/2+y, 1/4)$ and (4) $(1/2, 1/2-y, 3/4)$.

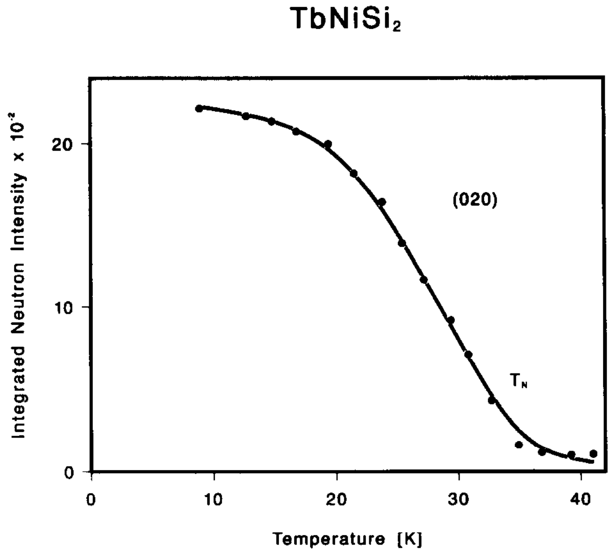

Fig. 4. Temperature dependence of the intensity of the magnetic 020 reflection for $TbNiSi_2$.

3. Concluding remarks

A schematic representation of the crystallographic and magnetic structure is given in Fig. 5. The collinear antiferromagnetic structure can be described by means of pairs of closely spaced ferromagnetically ordered planes of terbium atoms stacked antiparallel along the *b* direction. Within the ferromagnetic planes the terbium moments are oriented along the *c* direction. A similar magnetic structure was also observed in $HoCoSi_2$ [10], but for $TbCoSi_2$ a complex spiral type of structure was found. It is possible that this difference in behaviour is caused by the

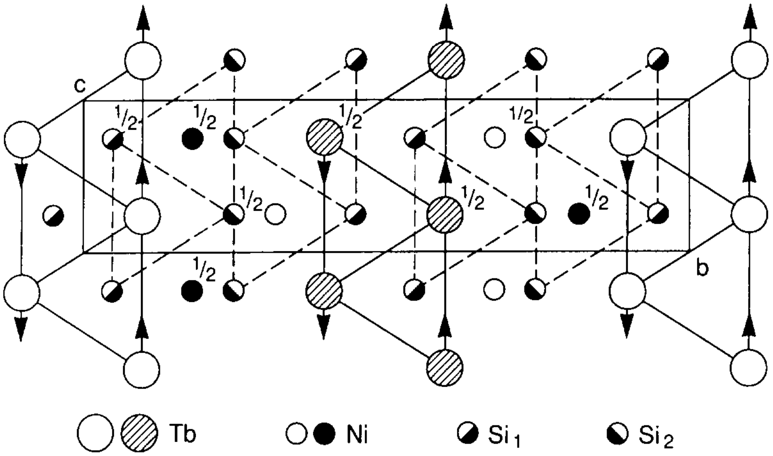

Fig. 5. Schematic representation of the crystallographic and magnetic structure of TbNiSi$_2$: ○, ○, atoms at $z = 0$; ▨, ●, ◐, ◑, atoms at $z = \frac{1}{2}$.

next-nearest-neighbour distance (associated with the intersublattice interaction) that is somewhat larger in TbCoSi$_2$ ($d_{12} = 0.4144$ nm) than in TbNiSi$_2$ ($d_{12} = 0.4012$ nm) whereas the nearest-neighbour distances (associated with the intrasublattice interaction) is almost equal in TbCoSi$_2$ ($d_{11} = c = 0.3972$ nm) and TbNiSi$_2$ ($d_{11} = c = 0.3961$ nm).

Preliminary investigations of the magnetic properties of RNiSi$_2$ compounds have shown that these properties are difficult to understand in terms of a unified model such as provided by the Ruderman–Kittel–Kasuya–Yoshida interaction. A more detailed study of these compounds by means of neutron diffraction is in progress.

Acknowledgment

The authors wish to express their gratitude to F. Cardi for performing the magnetic measurements.

References

1 O. P. Bodak and E. I. Gladyshevskii, *Sov. Phys. Crystallogr.*, *14* (1970) 859.
2 P. Schobinger-Papamantellos and K. H. J. Buschow, *J. Magn. Magn. Mater.*, *82* (1989) 99.
3 P. Schobinger-Papamantellos, D. B. de Mooij and K. H. J. Buschow, *J. Magn. Magn. Mater.*, *79* (1989) 231.
4 M. Francois, G. Venturini, B. Malaman and B. Roques, *J. Less-Common Met.*, *160* (1990) 197, 215.
5 H. M. Rietveld, *J. Appl. Crystallogr.*, *2* (1969) 65.
6 A. W. Hewat, *Harwell Rep. AERE-R7350*, 1973 (Atomic Energy Research Establishment, Harwell).

7 V. Sears, in K. Skoeld and D. L. Price (eds.), *Methods of Experimental Physics*, Vol. 23A, Academic Press, New York, 1986, p. 521.
8 A. J. Freeman and I. P. Desclaux, *J. Magn. Magn. Mater.*, *12* (1979) 11.
9 W. Opechovski and R. Guccione, in G. Rado and H. Suhl (eds.), *Treatise of Magnetism*, Vol. IIA, Academic Press, New York, 1965, p. 105.
10 A. Szytula, H. Ptasiewicz-Bak, J. Leciejewicz and W. Bazela, *J. Magn. Magn. Mater.*, *80* (1989) 189.